AJNR

Evaluation of the circle of Willis with three-dimensional CT angiography in patients with suspected intracranial aneurysms.

R A Alberico, M Patel, S Casey, B Jacobs, W Maguire and R Decker

Evaluation of the Circle of Willis with Three-dimensional CT Angiography in Patients with Suspected Intracranial Aneurysms

Ronald A. Alberico, Mahendra Patel, Sean Casey, Betsy Jacobs, William Maguire, and Robert Decker

PURPOSE: To determine the usefulness of CT angiography in the setting of suspected acute subarachnoid hemorrhage or intracranial aneurysm. **METHODS:** We prospectively studied 68 patients suspected of having subarachnoid hemorrhage or an intracranial aneurysm with noncontrast CT of the head followed immediately by contrast-enhanced helical CT of the circle of Willis with three-dimensional reconstruction. Twenty-seven patients with CT findings positive for subarachnoid hemorrhage or intracranial aneurysm were evaluated with digital subtraction angiography or MR angiography within 12 hours of CT angiography. Patients with negative CT/CT angiography findings were followed up with lumbar puncture. **RESULTS:** CT angiography showed 23 of 24 aneurysms and 2 of 2 arteriovenous malformations (sensitivity, 96%; specificity, 100%). Aneurysm size ranged from 2 to 40 mm (mean, 7.9 mm). Interobserver variability was 10%. In the 23 cases of subarachnoid hemorrhage, cisternal blood did not limit the three-dimensional reconstruction. Two patients with aneurysms on CT angiography had normal noncontrast scans. **CONCLUSIONS:** CT angiography of the circle of Willis is a useful technique for evaluation of suspected acute subarachnoid hemorrhage and intracranial aneurysm. It provides anatomic display of intracranial aneurysms, allowing for planning of conventional angiography and surgical approach. In selected cases, CT angiography may eliminate the need for preoperative conventional angiography.

Index terms: Aneurysm, intracranial; Computed tomography, three-dimensional; Subarachnoid space, hemorrhage

The workup of patients with suspected subarachnoid hemorrhage routinely includes initial noncontrast computed tomography (CT) followed by lumbar puncture if the CT findings are negative. Further study of patients with proved subarachnoid hemorrhage includes conventional angiography and/or magnetic resonance (MR) angiography to search for intracranial aneurysms or other potential causes of acute subarachnoid hemorrhage.

Although conventional angiography is the standard of reference for evaluating the intracranial vasculature, it poses some problems in the setting of acute subarachnoid hemorrhage. Time is required to assemble the angiography team and perform the angiogram. Time delays can have a significant effect on the course of a critically ill patient. Furthermore, conventional angiography has a finite risk of vascular complications including hematoma, vascular spasm, and stroke.

MR angiography has been proved efficacious in evaluating the cerebral vasculature (1–6). MR angiography offers the advantages of multiplanar and three-dimensional reconstruction without intravenous contrast or ionizing radiation. MR angiography, however, in the setting of acute subarachnoid hemorrhage, is frequently impractical and cannot always be performed on intubated patients or those with ferromagnetic aneurysm clips (7). MR angiography also is limited in the evaluation of aneurysms with turbulent or low flow (8).

The advent of helical computed tomography (CT) imaging has resulted in new techniques for evaluating vascular lesions using CT angiography (9–12). CT angiography of the circle of Willis has proved to be an effective means of evaluating aneurysms and adds little additional time to the routine CT examination (13). We prospectively evaluated the usefulness of CT angiography of the circle of Willis in the workup of patients with suspected acute subarachnoid hemorrhage or intracranial aneurysm. Previous retrospective studies comprise 9 patients with acute subarachnoid hemorrhage (12, 13).

Methods

From June 1994 to March 1995, 68 consecutive patients presented with clinically suspected acute subarachnoid hemorrhage or suspected intracranial aneurysm based on signs of cranial nerve compression. Severity of clinical symptoms was graded on the Hunt/Hess scale of 1 through 5 (14). All clinical grades were included in the study. Patient ages ranged from 9 to 88 years. The patients were evaluated with noncontrast CT examination followed immediately by 3-D CT angiography using a General Electric Hi-Speed Advantage Spiral CT scanner with Advantage Windows 3-D workstation (General Electric, Milwaukee, Wis). Conventional angiography was performed in the 24 patients with abnormality demonstrated on the CT angiography within 12 hours of the initial study. Three patients were evaluated with CT angiography followed by MR angiography using 3-D time-of-flight technique on a 1-T mobile GE Signa Magnet (General Electric, Milwaukee, Wis). Two CT angiograms were made after conventional angiograms, one of which was interpreted by a reader blinded to the result and existence of the prior angiogram. Five CT angiograms were done on patients with suspected acute subarachnoid hemorrhage and intracranial aneurysm clips from previous neurosurgery. Five of the patients who had CT angiography were intubated during the examination.

Noncontrast CT scans were performed with 5-mm contiguous axial sections through the posterior fossa followed by 10-mm contiguous axial sections to the vertex. CT angiography was performed using an injection of nonionic contrast at a rate of 3 mL/s for 80 mL initiated with a 15-second prescan delay. A 1-mm collimated helical scan with a 1:1 pitch was obtained from the cavernous carotid cephalad for at least 3.5 cm. On average, a total dose of 24 g of iodine was administered. Nonionic contrast was used to decrease the potential for minor reactions and thus for patient motion.

Scan duration was 35 to 42 seconds in all cases. Display field of view was set to 15 cm centered on the circle of Willis. Images were reconstructed using visual thresholding to remove bone without deleting vascular structures. Upper thresholds varied from 230 to 364 HU in the first phase of reconstruction. First-phase images included a large perivascular margin of soft tissue and were optimized manually by the radiologist. Optimization was performed by decreasing the lower threshold limit until the vessels were completely included in the image and then decreasing the threshold by an additional 5 to 10 HU to include perivascular soft tissue. Fine tuning of the final model was completed by filtering discontinuous groups of pixels (floaters) of 2.5 pixels or less in size. Portions of the skull base that remained after the threshold and filtering steps were removed manually. Average reconstruction time was 15 minutes. The total examination time did not exceed 30 minutes including 3-D reconstruction.

Maximum intensity projection is the algorithm that we used to display the 3-D images. It assigns an intensity to each pixel on the screen that is the maximum of all intensities in the 3-D model along a perpendicular line through that pixel. This display technique enabled us to see the vessel through the perivascular margin of soft tissue that we included in the threshold step.

For statistical purposes, CT angiography findings in 24 cases were compared with conventional angiography and 3 with MR angiography. Conventional angiography was performed with digital subtraction technique using the standard anteroposterior, lateral, and oblique views. All four vessels were studied. Additional views were obtained based on the CT angiography projection that best showed the aneurysm neck. MR angiography was performed using 3-D time-of-flight sequences over a 60-mm volume gradient echo (40–50/5–10/1 [repetition time/echo time/excitation]; flip angle, 20°). Images for filming were selected by the radiologist reviewing the case.

Three radiologists, one very experienced, one moderately experienced, and one with no previous experience with CT angiography, independently reconstructed and interpreted 48 of the exams. Only one or two radiologists interpreted the other exams. Each radiologist interpreted his or her own reconstructed images. Although this process combined interobserver variability (image interpretation) and interoperator variability (image reconstruction) into a single term, we feel it most closely paralleled the clinical situation.

The most experienced reader interpreted the CT angiography before the angiogram in all but two cases. The other observers were blinded to the result and existence of the angiogram in all cases. All three observers interpreted 48 cases, which included 26 positive cases and 22 negative cases. All three observers had knowledge of the emergency department history as it was stated on the request and of the noncontrast CT results. Eight data points were scored per case representing each vessel in the circle of Willis. Values from 1 to 5 were assigned for each data point representing the range from definitely normal, 1, to definitely abnormal, 5. For the purposes of positive and negative correlation, the values 1 and 2 were considered negative, 3 was equivocal, and 4 and 5 were positive.

Aneurysm size was measured directly using the CT software calipers. Comparisons were made to measurements made manually from the digital subtraction angio-

TABLE 1: Thirty cases in which abnormality was shown on CT angiography

Patient	Indication	Subarachnoid Hemorrhage Grade*	Subarachnoid Hemorrhage on CT†	CT angiography findings				
				Lesion Type	Location‡	Size, mm	Interpretation by Reader 1/2/3†§	Neck†
1	Coma	5	+	Aneurysm	ACOM	3		−
2	Coma	5	+	Aneurysm	ACOM	3.2	+/+/+	+
3	Headache	2	+	Aneurysm	R MCA	6.3	+/+/+	+
4	Seizure	4	+	Aneurysm	R PCOM	8.5	+/+/+	+
5	Headache	2	+	Aneurysm	L MCA	3.9	+/+/+	+
6	Headache	2	+	Aneurysm	R PCOM	2	+/−/−	+
7	Headache	2	+	Aneurysm	L PCOM	2	+/+/+	+
8	Headache	1	−	Aneurysm	L MCA	5.3	+/+/+	+
9	Headache	2	+	Aneurysm	R PCOM	13	+/+/−	+
10	Headache	1	+	Aneurysm	R PCOM	2	−/−/−	+
11	Headache, emesis	3	+	Aneurysm	R MCA	3	+/+/+	+
12	Headache, lethargy	3	+	Aneurysm	Internal carotid artery/MCA	11	+/+/+	−
13	Headache	1	+	Aneurysm	L MCA	2	+/+/+	+
14	Headache, emesis	3	+	Aneurysm	R PCOM	5.9	+/+/+	+
15	Headache	2	−	Aneurysm	ACOM	10	+/+/+	+
16	Headache	2	+	Aneurysm	R PCOM	3	+/+/+	+
17	Headache	1	+	Aneurysm	L MCA	3.1	+/+/+	+
18	Headache	2	+	Aneurysm	Basilar	2	+/+/+	+
19	Headache	2	+	Aneurysm	ACOM	15	+/+/+	+
20	Headache	1	+	Aneurysm	ACOM	7	+/+/+	+
21	Headache, emesis	3	+	Aneurysm	Internal carotid artery/MCA	12	+/+/+	+
22	Headache	2	+	Arteriovenous malformation	Frontal	. . .	+/. . ./. . .	. . .
23	Headache	1	−	Arteriovenous malformation	Large frontal	. . .	+/+/+	. . .
24	Headache	2	+	Pituitary mass	No aneurysm confirmed on digital subtraction angiogram			
25	Headache	1	+	No aneurysm on CT angiography or digital subtraction angiograms				
26	7th nerve compressed	. . .	−	Aneurysm	R MCA	40	+/+/+	+
27	Headache	1	−	Aneurysm	R anterior cerebral artery	19	+/+/+	+
28	Headache	2	−	Sinus thrombosis	. . .	. . .	. . .	. . .
29	Headache	2	−	Sinus thrombosis	. . .	. . .	. . .	. . .
30	Headache	2	+	Aneurysm	ACOM	13	+/+/+	+

* Hunt and Hess classification (14).

† Plus sign indicates present on the study; minus sign, not present.

‡ACOM indicates anterior communicating artery; MCA, middle cerebral artery; and PCOM, posterior communicating artery.

§ Readers 1 and 2 are the experienced and moderately experienced observers, and reader 3 is the inexperienced observer.

grams. Because magnification was not calculated on the digital subtraction angiograms, a ratio of the aneurysm size to its vessel of origin was made on both the CT angiogram and digital subtraction angiogram on similar views and in the same anatomic locations. This aneurysm index was used to assess correlation of aneurysm size between the two studies. All statistics were performed on a PC-based version of SPSS software. The detection of an aneurysm neck was assessed visually. A neck was considered to be present if an aneurysm narrowed to 50% or less of its maximum transverse diameter at the site of attachment to its vessel of origin.

Results

Of 68 cases prospectively evaluated, there were 66 cases with suspected acute subarachnoid hemorrhage and 2 cases with signs of cranial nerve compression and suspected intracranial aneurysm. CT angiography showed an abnormality in 30 cases (Table 1). Twenty-three cases were positive for acute subarachnoid hemorrhage, including 20 aneurysms. Cases without acute subarachnoid hemorrhage

TABLE 2: Interobserver variability of reported aneurysms*

| Observer | No. of aneurysms reported (average score given for middle cerebral/posterior communicating/anterior communicating arteries[†]) | | | |
	True-Positives	True-Negatives	False-Positives	False-Negatives
1	23 (5/4.7/5)	2 (1/1/1)	0 (. . .)	1 (. . ./2/. . .)
2	22 (5/4.7/5)	2 (1/1.1/1)	1 (4/. . ./. . .)	2 (. . ./2.5/. . .)
3	21 (5/4.4/5)	2 (1/1.3/1)	0 (. . .)	3 (. . ./1.7/. . .)

  * Observers 1 and 2 are experienced and observer 3 is relatively inexperienced. The results are for interpretation of cases with digital subtraction angiography or MR angiography correlation.

  † Average scores for the three most commonly abnormal vessels are listed for each observer in all categories. A score of 1 was definitely normal, a score of 5 definitely abnormal.

included 4 with aneurysms, for a total of 24 aneurysms detected with CT angiography.

Lumbar puncture was performed in 33 of the 44 negative cases and failed to demonstrate subarachnoid blood in 32 of these cases. In the remaining case, the cerebrospinal fluid was xanthochromic after centrifugation. Follow-up MR angiography of this case failed to demonstrate an intracranial aneurysm. This patient refused conventional angiography.

Interclass correlation among the three observers was 90%. Positive agreement and negative agreement were 77% and 98%, respectively. When the inexperienced observer was eliminated, positive agreement increased to 87%. For aneurysms larger than 2 mm, the positive agreement between the experienced observers was 100%. CT angiography was 95% sensitive and 100% specific for the most experienced observer. The moderately experience observer was 90% sensitive and 97% specific, and the inexperienced observer was 85% sensitive and 100% specific (Table 2).

In the one case in which the aneurysm was missed by all three observers, it measured 2 mm, and the contrast injection rate had to be decreased to 2 mL/s because of patient discomfort. No other contrast-related side effects occurred during the study.

There were six anterior communicating artery aneurysms (Fig 1), seven posterior communicating artery aneurysms (Fig 2), seven middle cerebral artery aneurysm (Fig 3), two internal carotid bifurcation aneurysms, one anterior cerebral artery aneurysm, and one basilar tip aneurysm. Minimum aneurysm size detected was 2 mm and size ranged from 2 to 40 mm, with an average of 7.9 mm. Aneurysm index as described in "Methods" failed to show statistical difference between CT angiography and digital
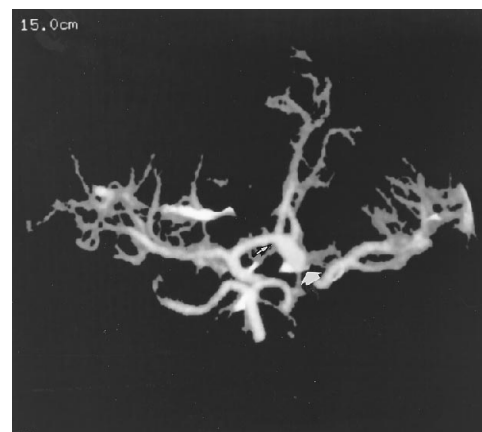
A
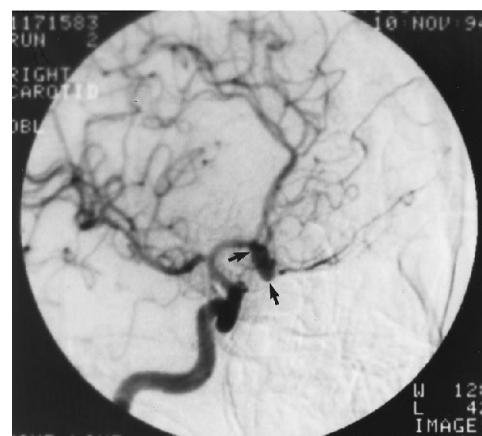
B

Fig 1. *A*, CT angiography demonstrates a 10-mm anterior communicating artery aneurysm (*large arrow*) with clear delineation of the neck (*small arrow*).

B, Oblique digital subtraction angiogram from a right internal carotid injection was planned using the CT angiography image. Excellent views of the aneurysm and neck were obtained in the first run (*arrows*).
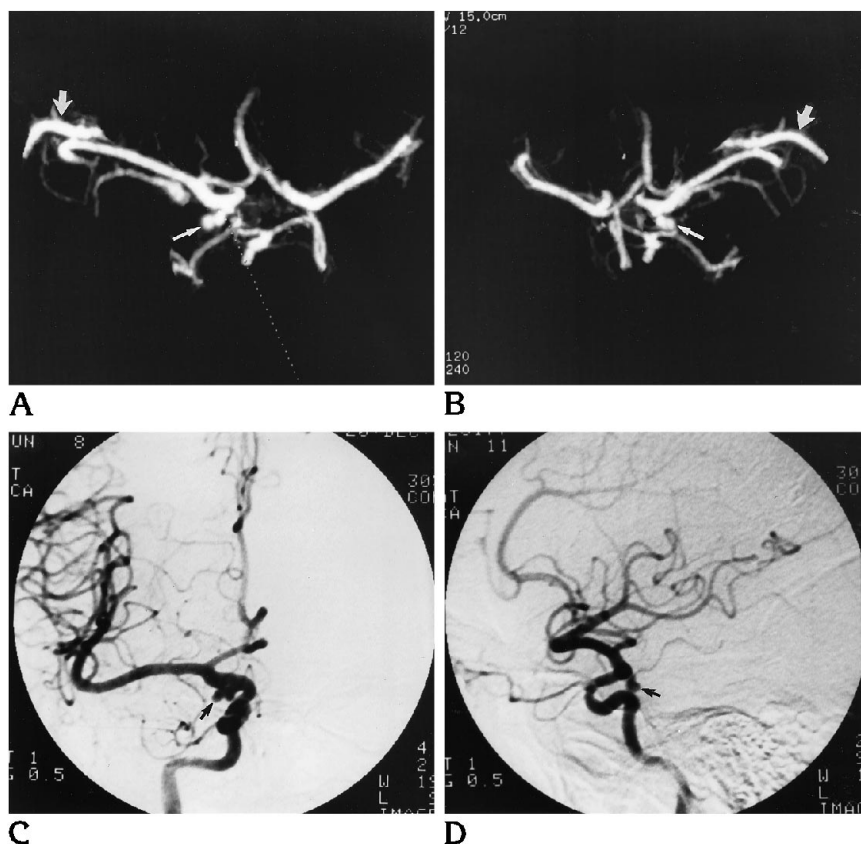
Fig 2. *A* and *B*, The lobulated right posterior communicating artery aneurysm is well seen on the CT angiogram (*arrows*). The inclusion of a vein in the reconstructed image (*large arrow*) demonstrates a limitation of CT angiography in its ability to discriminate the venous from arterial phase of the contrast bolus.

C and *D*, Lateral and anteroposterior digital subtraction angiography views after right internal carotid injection also demonstrate the lobulated nature of the aneurysm (*arrows*).

subtraction angiography as measured by a standard *t* test [$t(14) = .19$; $r = .95$]. The aneurysm neck was clearly demonstrated in 22 of 24 cases on both the CT angiography and the digital subtraction angiography.

Incidentally noted abnormalities included two sagittal sinus thromboses and two pituitary masses. In two cases of acute subarachnoid hemorrhage, arteriovenous malformations were detected on CT angiography.

Discussion

Previous retrospective studies have demonstrated the efficacy of CT angiography in evaluating patients with known cerebral aneurysms; however, only 9 of the patients had acute subarachnoid hemorrhage in these studies (12, 13). Our prospective series of 68 patients includes 23 patients with acute subarachnoid hemorrhage. The increased attenuation of acute
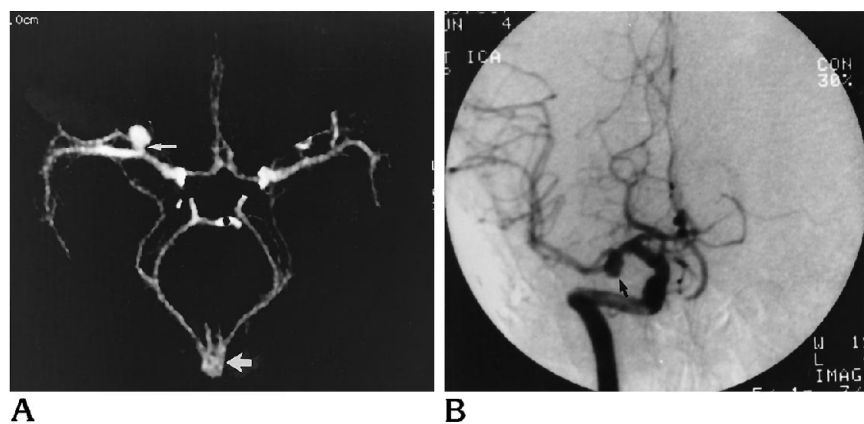
Fig 3. *A*, Inferior view CT angiogram demonstrates a right middle cerebral artery aneurysm with excellent evaluation of the aneurysm neck (*arrow*). A part of the straight sinus was included in this reconstruction (*large arrow*).

B, Anteroposterior view after right internal carotid injection clearly shows the inferiorly oriented right middle cerebral artery aneurysm (*arrow*). The inferior orientation was shown on other views from the CT angiography.

Fig 4. *A*, This posterior communicating artery aneurysm was missed by the experienced observer (*arrow*).

B, A retrospectively reconstructed model improves conspicuity of the aneurysm (*arrow*).

C and *D*, Digital subtraction angiography images in the anteroposterior and lateral projection after left internal carotid injection demonstrate the PCOM aneurysm clearly (*arrows*).
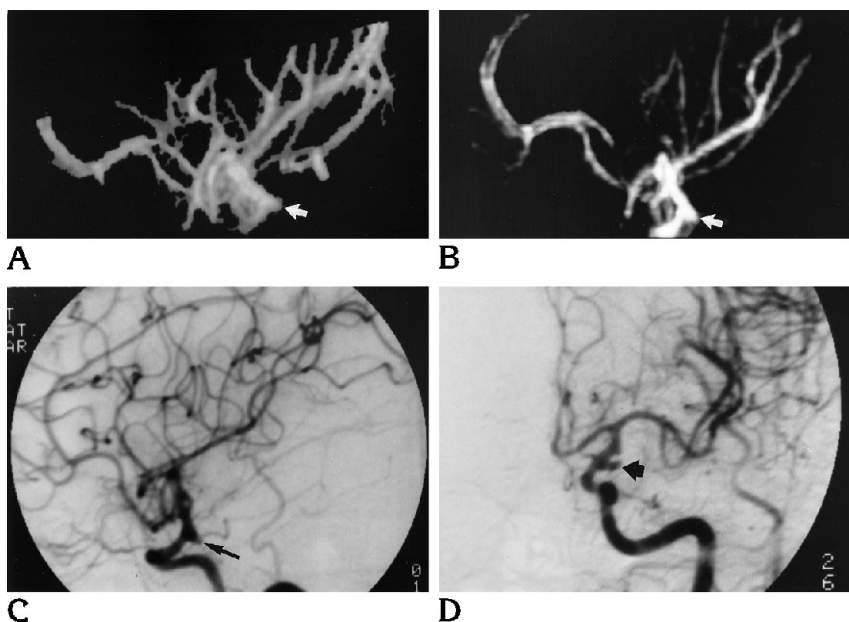
subarachnoid blood and enhanced vessels had no effect on our ability to define the vessels during 3-D reconstruction. In our series, cisternal blood measured between 80 and 120 HU lower than the enhanced vessels in all cases. This level of contrast was more than adequate for isolation of vessels in all of our reconstructions.

False-positive and false-negative results in this series resulted from difficulties in separating contrast-enhanced vessels from the skull base. The small posterior communicating artery aneurysms (2 mm) were more difficult to demonstrate because of their proximity to the internal carotid artery and skull base. This was apparent in the number of errors that occurred in evaluating the posterior communicating artery, particularly with the inexperienced observer (Fig 4).

The middle cerebral artery aneurysms were demonstrated best, making direct measurement of the aneurysm neck and diameter easy (Fig 3). No errors were made in identifying middle cerebral artery aneurysms. Most data points for the middle cerebral artery were scored either 1 (definitely normal) or 5 (definitely abnormal) by all three observers, suggesting a high level of confidence in evaluating this vessel (Table 2). The anterior communicating artery also was well visualized in all cases, and aneurysms were easily detected.

Difficulty in separating the veins from arteries resulted, at times, from their simultaneous enhancement (Fig 2). Although this simultaneous enhancement occasionally caused unwanted overlapping structures in certain views, it did not pose a problem in evaluating the circle of Willis for aneurysms. Two cases of sagittal sinus thrombosis seen in the periphery of the CT angiography source images were detected because of this simultaneous enhancement.

Advantages of CT angiography over MR angiography in the acute setting include decreased time to diagnosis. Total time required for the CT angiography examination and reconstruction was less than 30 minutes in all cases and less than 15 minutes in most. The quality of the images in CT angiography is less impaired by patient motion than in MR angiography because of the more rapid acquisition of CT images. MR angiography cannot always be used in intubated patients or in patients with ferromagnetic intracranial vascular clips. Frequently, the type of intracranial vascular clip cannot be verified by history in patients presenting with acute subarachnoid hemorrhage, and thus MR angiography cannot be performed (7). MR angiography may miss aneurysms with low or turbulent flow.

Advantages of MR angiography include the lack of intravascular contrast material and ionizing radiation. Sequences can be repeated if necessary to obtain optimal images when initial attempts fail because of patient motion or technical failure. Additionally, the volume of reconstruction in MR angiography is greater than in
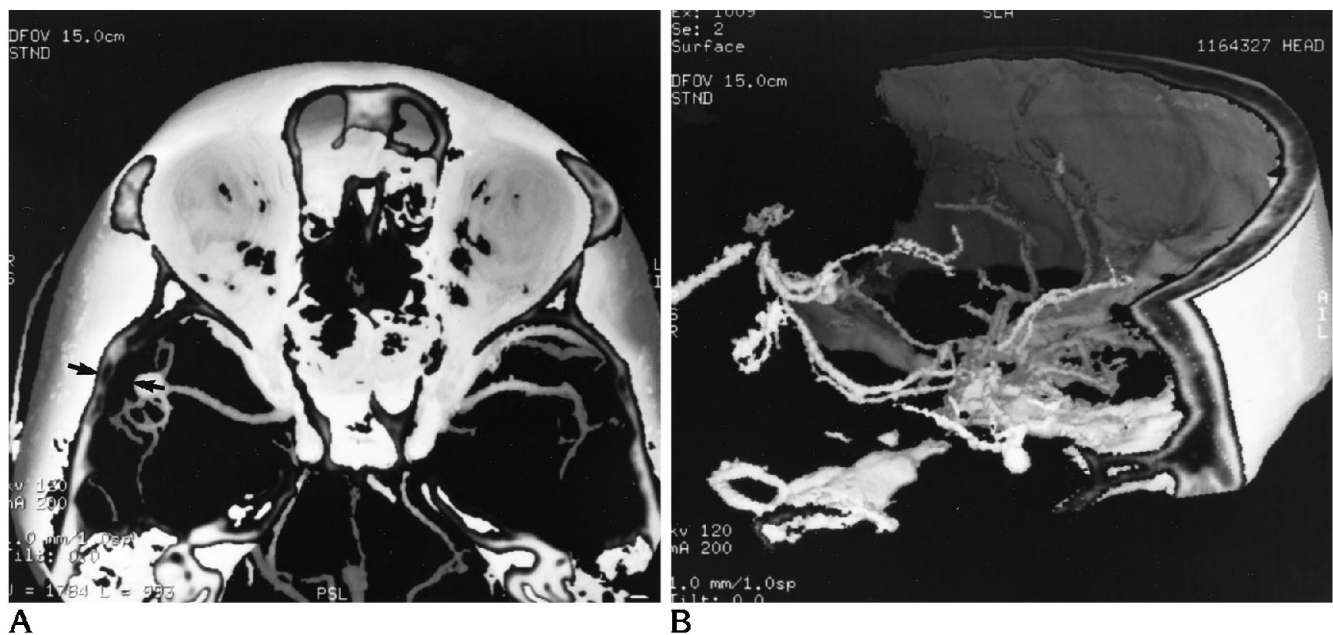
Fig 5. CT angiography allows the 3-D shaded surface display of bone landmarks, which provides for improved surgical planning. The relationship of this right middle cerebral artery aneurysm to the inner table of the skull is well shown (*A, arrow*), as is its orientation after computerized temporal craniotomy (*B*).

CT angiography, enabling inclusion of the vertebral arteries in the images.

Advantages of CT angiography over conventional angiography include decreased cost, invasiveness, and time to diagnosis. Patients can be evaluated immediately after the diagnosis of subarachnoid hemorrhage is made. CT angiography also allows the display of adjacent bone landmarks in 3-D for surgical planning (Fig 5). After CT angiography, conventional angiography can be tailored to enable more rapid and thorough evaluation of the lesion. The aneurysm neck was seen equally well in the CT angiogram and the digital subtraction angiogram.

Although CT angiography showed high specificity and sensitivity in our series, some limitations became apparent. CT angiography falls short of conventional angiography and MR angiography in evaluating large vascular territories. We initially attempted to evaluate large vascular territories in an effort to include the vertebral arteries in our 3-D models. The additional information made 3-D reconstruction difficult because of the presence of multiple overlapping structures. Further study may reveal that segmental reconstruction of large helical scans can resolve this problem.

The 3-D reconstruction process is operator-dependent. Improper thresholding can markedly alter the appearance of the vessels and could potentially result in elimination of vascular branches or aneurysms (15). Visual thresholding individualized to each case in conjunction with maximum intensity projection reconstruction resolved these problems in our series. Aneurysms missed by the least experienced observer all were related to the posterior communicating artery. Errors resulted from failure to review the axial images before the reconstruction. Axial images must be reviewed so that the inferior and superior extent of the 3-D model is sure to include all of the vessels of interest.

Although our series was correlated with digital subtraction angiogram images, from which no exact aneurysm size could be obtained, there was no significant difference in the aneurysm index measurement between the two studies. Therefore, one can conclude that direct measurements on the CT angiogram are likely to be accurate. Comparison with cut-film angiography is required to be certain. Given the current data, 2 mm may represent the lower limit of aneurysm size detectable with this technique.

Of note in our series are two patients referred from the emergency room for suspected subarachnoid hemorrhage who had normal non-

contrast CT findings and aneurysms on CT angiography. We feel that this is an attractive argument for the use of CT angiography as a screening tool in these patients. The addition of post–CT angiography contrast CT as part of the screening protocol may increase the detection of incidental dural sinus thrombosis. This information could be important because dural sinus thrombosis may present with the same symptoms as subarachnoid hemorrhage.

In conclusion, 3-D CT angiography of the circle of Willis is a useful way of evaluating patients with suspected acute subarachnoid hemorrhage or intracranial aneurysm. It offers identification and characterization of aneurysms and is easily performed immediately after the initial noncontrast CT. Although some limitations occur because of operator-dependent 3-D reconstruction and limited evaluation of vascular territories more than 4 cm in superior/inferior extent, it promises to be an effective diagnostic test. In selected cases, preoperative angiography may not be needed after CT angiography.

References

1. Curnes JT, Shogry MEC, Clark DC, Elsner HJ. MR angiographic demonstration of an intracranial aneurysm not seen on conventional angiography. *AJNR Am J Neuroradiol* 1993;14:971–973
2. Schnierer G, Huk NJ, Laub G. Magnetic resonance angiography of intracranial aneurysms: comparison with intra-arterial digital subtraction angiography. *Neuroradiology* 1992;35:50–54
3. Gouliamos A, Gotsis E, Vlahos L, et al. Magnetic resonance angiography compared to intra-arterial digital subtraction angiography in patients with subarachnoid hemorrhage. *Neuroradiology* 1992;35:46–49
4. Heinz RE. Aneurysms and MR angiography. *AJNR Am J Neuroradiol* 1993;14:974–977
5. Sevick RJ, Tsuruda JS, Schmalbrock P. Three-dimensional time-of-flight MR angiography in the evaluation of cerebral aneurysms. *J Comput Assist Tomogr* 1990;14(6):874–881
6. Ross JS, Masaryk TJ, Modic MT, et al. Intracranial aneurysms: evaluation by MR angiography. *AJNR Am J Neuroradiol* 1990;11:449–456
7. Klucznik NP, Carrier DA, Pyka R, Haid RW. Placement of a ferromagnetic intracerebral aneurysm clip in a magnetic field with a fatal outcome. *Radiology* 1993;187:855–856
8. Masaryk TJ, Modic MT, Ross JS, et al. Intracranial circulation: preliminary results with three-dimensional (volume) MR angiography. *Radiology* 1989;171:793–799
9. Dillon HE, VanLeeuwen MS, Fernandez MA, Mali WP. Spiral CT angiography. *AJR Am J Roentgenol* 1993;160:1273–1278
10. Schmid UD, Steigen HJ, Huber P. Accuracy of high resolution computed tomography in direct diagnosis of cerebral aneurysms. *Neuroradiology* 1987;29:152–159
11. Napel S, Marks MP, Rubin GD, et al. CT angiography with spiral CT and maximum intensity projection. *Radiology* 1992;185:607–610
12. Schwartz RB, Tice HM, Hooten SM, et al. Evaluation of cerebral aneurysms with helical CT: correlation with conventional angiography and MR angiography. *Radiology* 1994;717–722
13. Aoki S, Sasaki Y, Machida T, et al. Cerebral aneurysms: detection and delineation using 3-D-CT angiography. *AJNR Am J Neuroradiol* 1992;13:1115–1120
14. Hunt WE, Hess RM. Surgical risk as related to time of intervention in the repair of intracranial aneurysms. *J Neurosurg* 1968;28:14–20
15. Zeman RK, Davros WJ, Berman P, Weltman DI, et al. Three-dimensional models of the abdominal vasculature based on helical CT: usefulness in patients with pancreatic neoplasms. *AJR Am J Roentgenol* 1994;162:1425–1429